Post-hurricane forest damage assessment using satellite remote sensing

Wanting Wang [a,*], John J. Qu [a], Xianjun Hao [a], Yongqiang Liu [b], John A. Stanturf [b]

[a] EastFIRE Lab, Environmental Science and Technology Center (ESTC), College of Science, George Mason University, 4400 University Drive MS 6A2, Fairfax, VA 22030, USA
[b] Center for Forest Disturbance Science, US Forest Service, Athens, GA 30602, USA

ABSTRACT

This study developed a rapid assessment algorithm for post-hurricane forest damage estimation using moderate resolution imaging spectroradiometer (MODIS) measurements. The performance of five commonly used vegetation indices as post-hurricane forest damage indicators was investigated through statistical analysis. The Normalized Difference Infrared Index (NDII) was identified as the optimal damage indicator among these vegetation indices. An approach for detecting forest damage at a regional scale, without relying on ground inventory or sampling, was designed and validated. The validation showed that the relative change of pre- and post-hurricane NDII was linearly related to the damage severity estimated by the ground inventory with the coefficient of determination 0.79. This approach was applied to evaluate forest damage severity and the impacted region caused by Hurricane Katrina.

Published by Elsevier B.V.

1. Introduction

Hurricanes are one of the major natural disturbances to forest ecosystems in the southeastern United States. A severe hurricane can extensively influence the composition, structure and succession of forests, and consequently affect the terrestrial carbon sink (Foster, 1988; Boutet and Weishampel, 2003). From the perspective of fire management, the most immediate impacts of hurricanes are a massive conversion of living forest biomass to dead fuel (McNulty, 2002), an increase in fuel bed depth (Miranda, 1996), and decrease in dead fuel moisture (Gill et al., 1990; Loope et al., 1994). Previous studies have indicated that the occurrence and intensity of wildland fires increase in hurricane-impacted areas in the years after landfall (Gardner et al., 1991; Hook et al., 1991; Wade et al., 1993; Myers and van Lear, 1998; Liu et al., 2003).

The increased frequency and severity of resulting forest disturbances in recent years requires rapid and accurate regional forest damage assessment to support post-hurricane forest management, hazardous fuel management, post-hazard relief activities, and government compensation claims. Fuel loading is a key parameter in fire danger rating systems, which are not designed to assess increment of fire risk in hurricane-impacted forest regions. As a result, fixed fuel models in the National Fire Danger Rating System (NFDRS) (Schlobohm and Brain, 2002) introduce uncertainties in fire risk estimation due to the high spatial and temporal variability of hurricane-induced dead fuels.

Therefore, fuel models need to be adjusted to account for such variability, which require an efficient approach to measure abrupt fuel changes. Post-hazard relief activities (e.g. logging and fuel reduction) also require knowledge of the location and severity of forest damage to effectively carry out their missions (Stanturf et al., 2007). A map of forest damage severity also provides a objective evidence for verifying post-hurricane compensation claims and related government decisions.

Few studies have focused on satellite remote sensing of storm-induced forest damage. No operational, well tested and validated satellite remote sensing algorithm has been developed to rapidly assess post-hurricane forest damage and the severity in terms of defoliation, branch loss, stem loss and other changes in forest structure. Most studies to date have been based on passive optical remote sensing, in which the change or standardized change of various vegetation indices are adopted as damage indicators with few efforts to evaluate their quantitative relationship with forest damage at the pixel level, and with few comparative analyses on the performance of these vegetation indices. Studies on selecting a proper indicator for estimating post-hurricane forest damage have not been reported. Ramsey et al. (1997) analyzed forest damage caused by Hurricane Andrew 1992, using advanced very high-resolution radiometer (AVHRR) multi-temporal images. They found that the regional averaged Normalized Difference Vegetation Index (NDVI) change followed damage severity, but did not provide quantitative relation of NDVI change and damage severity. In their later research, they inferred that damage extent and information on damage severity and type might be extracted from the NDVI change (Ramsey et al., 1998). Ayala-Silva and Twumasi (2004) investigated forest damage caused by Hurricane Georges

* Corresponding author. Tel.: +1 703 994 1532; fax: +1 703 993 9299.
E-mail address: wwang@gmu.edu (W. Wang).

Table 1
Summary of studies on post-storm forest damage assessment.

Storm	Time	Sensors	Channels	Indicator	Change detection	Literature
Hurricane Andrew	08/1992	AVHRR	Red, NIR	NDVI	UID	Ramsey et al. (1997, 1998, 2001)
Hurricane Georges	09/1998	AVHRR	Red, NIR	NDVI	UID	Ayala-Silva and Twumasi (2004)
Typhoon Herb	07/1996	SPOT	Red, NIR	NDVI	UID	Lee et al. (2008)
Typhoon Songda	09/2004	ASTER	Red, NIR, SWIR	NDVI, NDII, LAI	UID	Aosier and Kaneko (2007)
Ice Storm	1994	Landsat TM	Red, NIR	NDVI	UID	Stueve et al. (2007)
Ice Storm	01/1998	Landsat TM	Red, NIR	NDVI	UID	Millward and Kraft (2004)
Partial Harvesting	2000-2004	Landsat TM	NIR, SWIR, Visible	NDVI, TCW	UID	Jin and Sader (2005)
Hurricane Katrina	08/2005	Landsat TM/MODIS	NIR, SWIR, Visible	Non-photosynthetic vegetation	Spectral mixture analysis	Chambers et al. (2007)
Hurricane Fran	09/1996	SLICER	NIR laser	Canopy height	–	Boutet and Weishampel (2003)
Hurricane Lothar	12/1999	ERS SAR	C-band (6 cm)	InSAR coherence	Classification	Dwyer et al. (1999) and Wiesmann et al. (2001)
		CARABAS-II SAR	VHF-band (3.3–15 m)	Backscattering amplitude	Linear regression	Fransson et al. (2002)

1998 using the standardized change of NDVI (ΔNDVI) derived from AVHRR images. They indirectly proved that regional averaged ΔNDVI was linearly related to the distance of the hurricane track. Aosier and Kaneko (2007) studied tree damage caused by Typhoon Songda 2004 using advanced spaceborne thermal emission and reflection radiometer (ASTER) images at local scale. They found that the NDVI change for damaged trees was greater than the change of adjusted Normalized Difference Infrared Index (NDII). Their finding was inconsistent with prior studies, in which vegetation modifications were better detected by NIR-SWIR based vegetation indices than NIR–Red based vegetation indices (e.g. Ceccato et al., 2001; Wilson and Sader, 2002; Sader et al., 2003; Bowyer and Danson, 2004; Jin and Sader, 2005).

The purpose of this paper is to evaluate the performance of commonly used vegetation indices in identifying post-hurricane forest damage, and to develop an algorithm to rapidly assess damage severity in hurricane-impacted forest regions. The specific objectives of this study are to (1) identify a reliable indicator for detecting impacted forest region and damage severity, (2) develop an algorithm for rapid post-hurricane damage assessment, and (3) validate this algorithm. In the next section, the approaches and satellite sensors used for detecting post-hurricane forest damage are reviewed. Datasets and methods are introduced in Section 3. Section 4 presents the results, including the identification of a proper damage indicator, development of a rapid assessment algorithm, and its application towards evaluating forest damage caused by Hurricane Katrina. Validation results are discussed in Section 5.

2. Existing approaches for estimating post-hurricane forest damage

The assessment of a hurricane-impacted forest region and forest damage severity has been traditionally based on the ground survey, aerial photography, ecological models, storm models, and topographic exposure models or combination of these methods (Sheffield and Thompson, 1992; Wade et al., 1993; Boose et al., 1994; Kovacs et al., 2001; McNulty, 2002; Clark et al., 2006; Jacobs, 2007; Kupfer et al., 2008; Wang and Xu, 2009). Research on satellite remote sensing of hurricane-induced forest damage started in the 1990s, because satellite data have high temporal and spatial resolution, and extensive coverage relative to ground and aerial measurements. The primary literature from peer-reviewed journals and government documents were summarized in Table 1. These previous approaches can be classified into four categories based on the respective physical principles used in detecting the forest canopy: (1) detection based on changes in chlorophyll content (Ramsey et al., 1997, 1998, 2001; Millward and Kraft, 2004; Ayala-Silva and Twumasi, 2004; Jin and Sader, 2005; Aosier and Kaneko, 2007; Stueve et al., 2007; Lee et al., 2008), (2)

detection based on changes in leaf water content (Jin and Sader, 2005; Aosier and Kaneko, 2007), (3) detection based on spectral mixture analysis (Chambers et al., 2007), and (4) detection based on structural changes of damaged forests (Dwyer et al., 1999; Wiesmann et al., 2001; Fransson et al., 2002; Boutet and Weishampel, 2003). Approaches in category 1 and 2 use NDVI, NDII, or variations of NDVI and NDII as damage indicators. The image differencing method is used to derive the change of damage indicators before and after a hurricane. Most studies adopted methods in category 1, since NDVI is a well-known and most popular vegetation index. Few studies are in category 2 despite much evidence indicating that NDII is more sensitive to vegetation modifications. Approaches in both categories are relatively simple, straightforward, and easy to implement and interpret for large-scale investigations. However, they are sensitive to errors in image geo-registration, sensor view geometry and vegetation phenology. NDVI is easier to saturate over dense canopies than NDII because red bands have weaker penetration capability than SWIR bands under the clear-sky condition. Since regions that are prone to the hurricane hazard usually have relatively dense canopies, NDVI-based indicators are more sensitive to the saturation problem. The application of spectral mixture analysis was reported by Chambers et al. (2007), which demonstrated a potential way to retrieve non-photosynthetic vegetation (i.e. wood, dead vegetation and surface litter). Their approach relied on the endmember classification based on high-resolution satellite data and field samples. Studies based on structural changes of post-hurricane forests are more preliminary. Synthetic Aperture Radar (SAR) coherence data has been shown effective on identifying forest and non-forest areas based on various classification techniques (Floury et al., 1997). However, few studies reported the quantitative assessment of post-hurricane forest damage.

3. Data and methods

3.1. Post-Hurricane Katrina field inventory in the De Soto National Forest

The De Soto National Forest (De Soto NF) is located in southern Mississippi. The De Soto NF encompasses 1532 km² (378,538 acres) of upland forest and bottomland forest, and is managed by the United States Department of Agriculture (USDA) Forest Service. The sub-tropical climate in the De Soto NF is characterized by mild, short winters and hot, humid summers (Kupfer et al., 2008). High precipitation is evenly distributed throughout the year. The topography is characterized by gently sloping uplands and floodplains.

The De Soto NF includes the Chickasawhay and De Soto Districts. Both of these districts are dominated by longleaf pine (*Pinus palustris*) forest, representing 44% of the forest cover
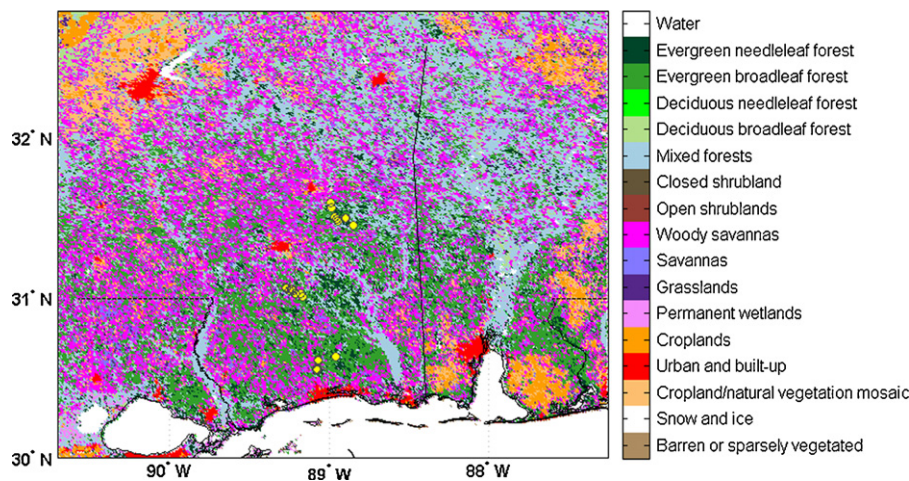
Fig. 1. Forest health evaluation stands and land cover type. Yellow dots are locations of Forest health evaluation stands. (For interpretation of the references to color in this figure legend, the reader is referred to the web version of the article.)

(Windham, 2005). Slash pine (*P. elliottiii*) and hardwood covers 23% and 8%, respectively. A combination of loblolly (*P. taeda*), shortleaf (*P. echinata*) and mixed yellow pine represents 14%. Pine and hardwood mixtures cover 10%. Bottomlands are dominated by hardwoods and sweetgum (*Liquidambar styraciflua*). Uplands are dominated by longleaf pine, loblolly pine, shortleaf pine and slash pine.

Hurricane Katrina landed as a category 3 hurricane with sustained wind speeds of 180–200 km h^{-1} on August 29 2005 in southeast Louisiana (Stanturf et al., 2007). Its eye passed within 8 km of the western boundary of the De Soto NF (Bryant and Boykin, 2007), and the storm's strong winds caused widespread forest damage in Mississippi. The USDA Forest Inventory Analysis (FIA) reported that 8300 km^2 National Forests in Mississippi were impacted. The De Soto NF suffered forest damage over 2270 km^2 of land. The De Soto NF experienced storm winds for several hours with maximum sustained winds averaging 135–160 km h^{-1} and peak gusts of 145–225 km h^{-1} (Kupfer et al., 2008).

The USDA Forest Service conducted forest health evaluation of the De Soto NF one month after the hurricane landfall. A total of 54 plots (405 m^2/0.1 acre per plot) within 18 separate stands were examined, which provided a representative range of hurricane damage from light to heavy levels (Meeker et al., 2006). The hurricane damage was then classified using four damage categories, including severe damage, moderate damage, light damage and no damage. The percentage of damaged trees in these four categories was calculated for each stand, and used as ground truth data in this study. The locations of these 18 stands are shown in Fig. 1 (yellow dots), overlaid with the MODIS IGBP land cover types (2004). The land pixels covered by evergreen needle-leaf forest, evergreen broadleaf forest, deciduous broad-leaf forest, mixed forests and woody savannas were studied in this research. Out of 54 plots, 20 plots were identified as evergreen needle-leaf forest; 22 plots were covered by evergreen broad-leaf forest; 1 plot was deciduous broad-leaf forest; 9 plots were dominated by mixed forests; and 2 plots were woody savannas.

3.2. MODIS products

The MODIS Nadir BRDF-Adjusted Reflectance (NBAR) Product (MOD43B4) contains visible and shortwave infrared (SWIR) surface reflectance adjusted to nadir views with a resolution of 1 km at the mean solar zenith angle of each 16-day period (Schaaf et al., 2002). This product provides the surface spectral reflectance

as it would have been measured at ground level without atmospheric scattering or absorption. The correction scheme used for the NBAR product compensated for the effects of atmospheric gases, aerosols and thin cirrus clouds. Since the BRDF and atmospheric effects have been removed from the MODIS NBAR product, the MODIS NBAR product is more stable and consistent than other reflectance products for observing vegetation status. Therefore, it is an optimal choice for monitoring vegetation change on land surfaces across broad spatial scales (Coppin et al., 2004). In this study, the MODIS NBAR product was adopted to derive NDVI, Enhanced Vegetation Index (EVI) and NDII. The Leaf Area Index (LAI) and Fraction of Photosynthetically Active Radiation (Fpar) in the MODIS LAI and FPAR product (MOD/MYD15A2) were used to derive the change of LAI and Fpar caused by hurricanes. Forest areas were identified by the IGBP land cover type in the MODIS land cover product (MOD12Q1). All these MODIS products were obtained from the LP DAAC, the EOS Data Gateway (EDG).

3.3. Change detection methods

One of the primary challenges to detecting large-scale abrupt vegetation modification is to eliminate or reduce errors caused by vegetation phenology (Zhang et al., 2003). Furthermore, variations caused by atmospheric effects, the BRDF effect and soil reflectance before and after change events constitute noise for detecting vegetation modification. Using the georegistered MODIS NBAR product eliminated most noise caused by atmospheric effects and BRDF effect. First, the CLEAN algorithm (Roberts et al., 1987; Baisch and Bokelmann, 1999), a nonlinear deconvolution approach based on Fourier transform theory, was used to fill in missing or low quality observations in the time series of vegetation indices (2003–2006) for each 1 km grid cell in the focus region.

Fig. 2 shows an example of estimated missing NDII observations within a NDII time series. The missing data were filled with the estimated values (solid dots) derived from the CLEAN algorithm. Then, the Fourier transform was used as a high-pass filter to separate phenological signals (low frequencies) and the signals caused by forest damage (high frequencies). Fig. 3 is an example of a complete NDII time series (solid line), its seasonal component (dash-dotted line) and the seasonally detrended disturbance component (dotted line). Finally, the seasonally detrended vegetation indices were subtracted using the Univariate Imaging Differencing (UID) method to derive the change in vegetation indices before and after a hurricane.
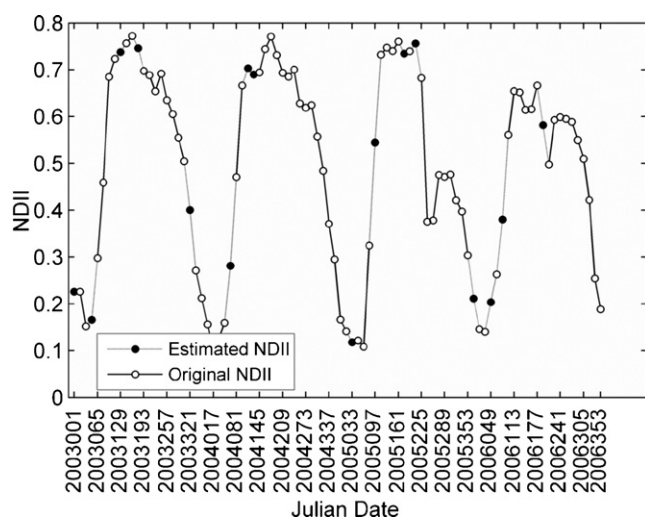
Fig. 2. Estimated missing NDII observations (solid dots) within an incomplete NDII time series.
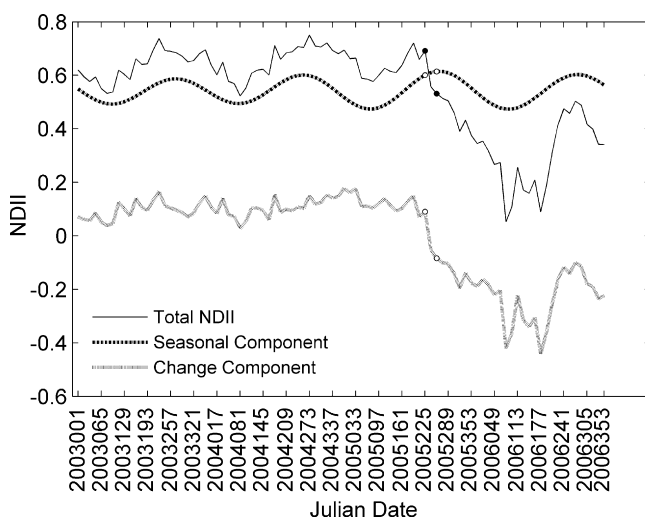

Fig. 3. Decoupling a NDII time series. Complete total NDII time series (solid line), its seasonal component (dash-dotted line) and the seasonally detrended disturbance component (dotted line).

The percentage of damaged tree pixels was derived for individual damage indicators (ΔVIs) to represent the overall performance of three vegetation indices. It was defined as the percentage of tree pixels with ΔVI values greater than the corresponding damage threshold. The damage thresholds were defined as $\overline{\Delta VI} + \delta$, where $\overline{\Delta VI}$ and δ were the respective mean and mean absolute deviation of ΔNDII, ΔNDVI or ΔEVI for undisturbed pixels within the impacted region (those within the red box in Fig. 4(a)) in 2003, 2004 and 2006. The undisturbed pixels were defined such that their ΔVIs were within the range of $\overline{\Delta VI}_{all} \pm \delta_{all}$, where $\overline{\Delta VI}_{all}$ and δ_{all} were the respective mean and mean absolute deviation of ΔNDII, ΔNDVI or ΔEVI for all pixels in the same region in 2003, 2004 and 2006. The mean absolute deviation was adopted as a measure of dispersion rather than the standard deviation because it was more resistant to outliers (Huber, 1981).

The damage level thresholds, which defined damage levels, were computed using the histogram of the damage indicator. Two thresholds were selected at first. Then, maps of damage indicator at three damage levels were separately inspected. The fourth damage level was then identified according to the spatial continuity of the selected three damage levels.

3.4. Commonly used vegetation indices

The NIR–Red spectra based vegetation index is the NDVI (Eq. (1)) or its variations, e.g. EVI (Eq. (2)):

$$NDVI = \frac{(NIR - Red)}{(NIR + Red)} \tag{1}$$

and

$$EVI = G \times \frac{(NIR - Red)}{(NIR + C_1 \times Red - C_2 \times Blue + L)} \tag{2}$$

where Red and NIR are the reflectance at 0.65 and 0.86 μm for MODIS, respectively; Blue is the reflectance at 0.47 μm for MODIS, and $C_1 = 1$, $C_2 = 7.5$, $L = 1$, $G = 2.5$. The NDVI separates green vegetation from other surfaces because of chlorophyll absorption in the red spectra and reflection in the NIR spectra (Tucker, 1979). Thus, high NDVI values indicate high leaf biomass, canopy closure, leaf area (Sellers, 1985; Jasinski, 1990) and the amount of photosynthetically active green biomass. NDVI cannot differentiate very dense canopy from dense canopy due to the limited penetration capability of reflected red spectra, which is referred to as the saturation problem. The Enhanced Vegetation Index (EVI) is based on chlorophyll absorption with a correction for the effect of atmosphere and soil reflectance (Huete et al., 1999). It is more sensitive than NDVI in high biomass regions. In Eq. (2), the aerosol resistance term used the blue band to correct for aerosol influences in the red band. By using the canopy background adjustment factor, L, the EVI is insensitive to most canopy backgrounds except for snow.

Estimation of vegetation water content typically utilizes signals from liquid water absorption channels in the SWIR spectra and contrasts them with signals from channels insensitive to liquid water in the NIR spectra. Several indices based on SWIR and NIR reflectance have been developed such as NDII (Eq. (3)) (Hardisky et al., 1983; Hunt and Rock, 1989):

$$NDII = \frac{(NIR - SWIR)}{(NIR + SWIR)} \tag{3}$$

where SWIR is the reflectance at 1.24, 1.65 or 2.13 μm for MODIS. Studies have shown that SWIR–NIR based indices are related to the weight of water per unit area, or the vegetation water content (Ceccato et al., 2001; Bowyer and Danson, 2004). In this study, we adopted the 2.13-μm channel, due to the large amount of missing observations caused by the serious stripping issue in the MODIS/Aqua 1.65-μm channel (Wang et al., 2006).

Leaf area index (LAI) is defined as one-sided leaf area per unit ground surface area for broadleaf trees, and half the total needle area per unit ground surface area for coniferous trees. This is a fundamental biophysical parameter that can connect the remotely sensed reflectance of green vegetation with leaf biomass in the canopy. The Fraction of Photosynthetically Active Radiation (Fpar) measures the proportion of available radiation in the photosynthetically active wavelengths (0.40–0.70 μm) that a canopy absorbs. LAI and Fpar can be remotely detected using MODIS and MISR (Knyazikhin et al., 1998a,b).

3.5. Identification of a proper damage indicator

Vegetation indices that have been used for estimating post-hurricane forest damage include NDVI, NDII, TCW (Tasseled Cap Wetness) and LAI. Most studies to date have adopted vegetation indices as damage indicators. Although various studies have shown that vegetation modification is better detected by vegetation indices based on the NIR–SWIR reflectance (Ceccato et al., 2001; Wilson and Sader, 2002; Sader et al., 2003; Bowyer and
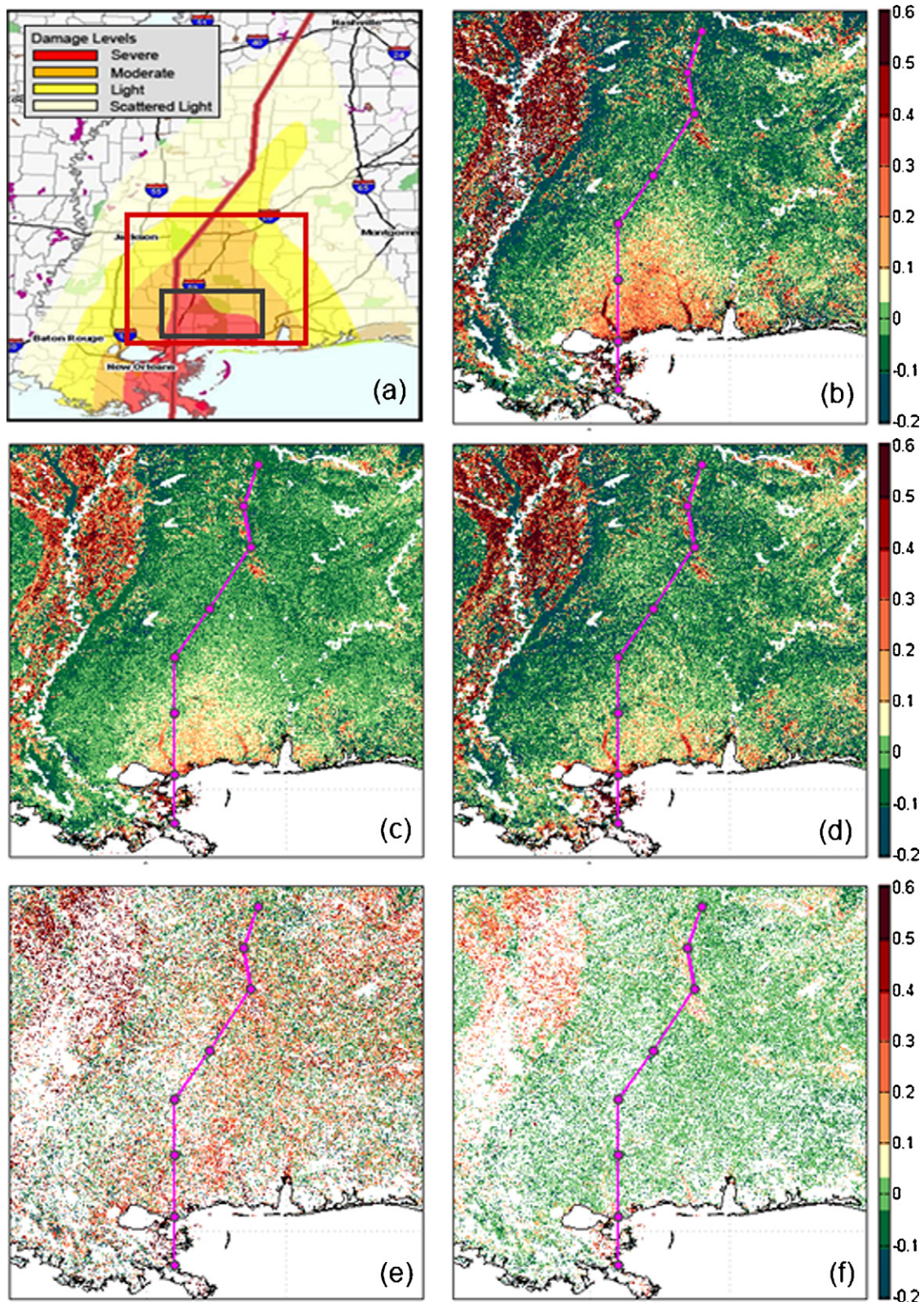
Fig. 4. Relative reduction of NDII, NDVI, EVI, LAI and Fpar before (August 13, 2005) and after (September 14, 2005) Hurricane Katrina. (a) Damage severity mapped by FIA, USDA Forest Service (Clark et al., 2006); (b) ΔNDII; (c) ΔNDVI; (d) ΔEVI; (e) ΔLAI; and (f) ΔFpar.

Danson, 2004; Jin and Sader, 2005), little research has been carried out to evaluate the sensitivity of commonly used vegetation indices for assessing hurricane-caused forest damage. Therefore, the performance of NDVI, EVI, NDII, LAI and Fpar was analyzed in this study. The Tasseled Cap Wetness (TCW) was not included in

the comparison because NDII and TCW are highly correlated ($R^2 > 0.98$) (Jin and Sader, 2005).

First, we compared the maps of relative reduction of seasonally detrended vegetation indices (ΔVIs) pre- and post-hurricane Katrina with the damage severity assessed by the USDA Forest
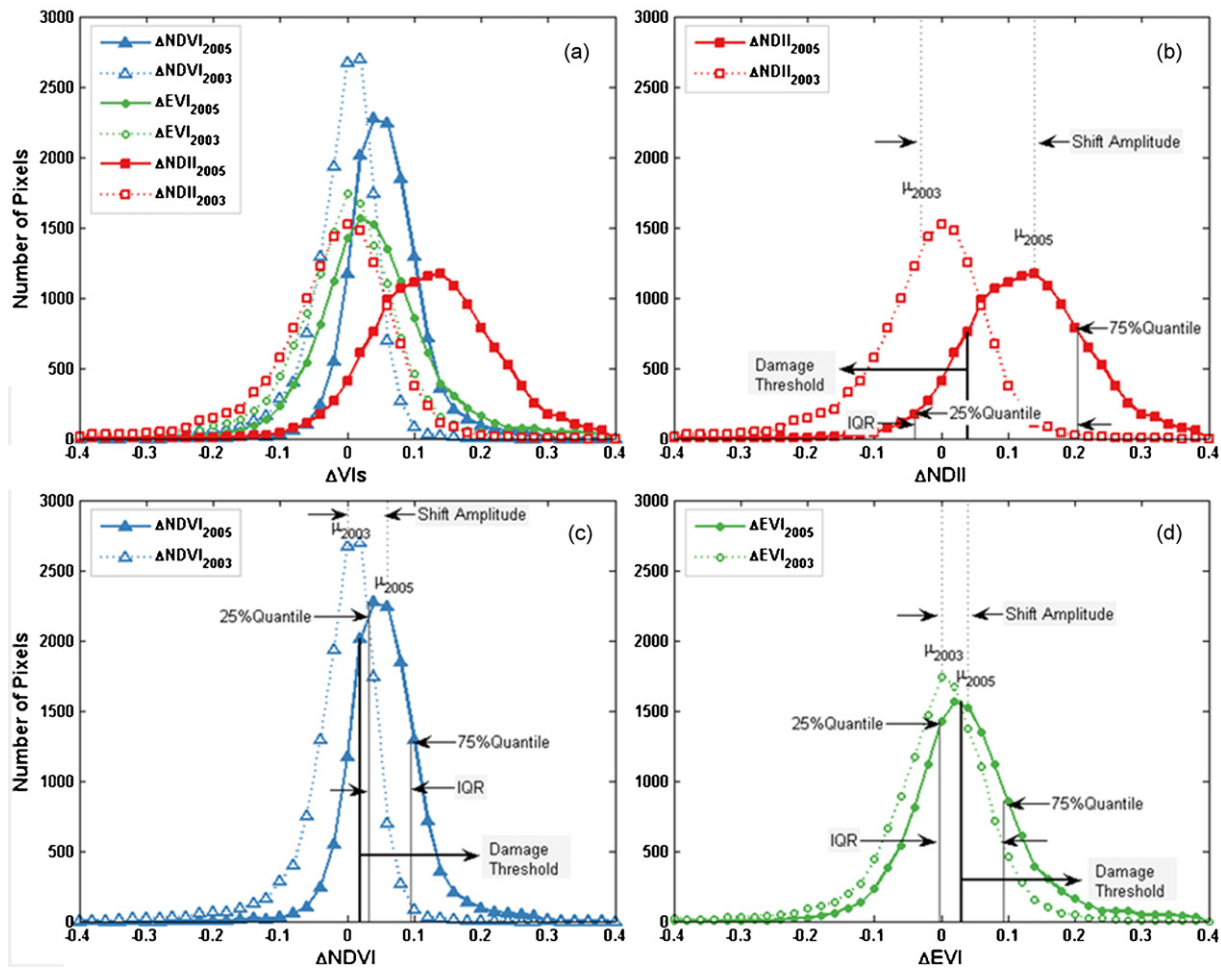
Fig. 5. Histograms of ΔVIs within the major impacted region, during August 13 and September 14, 2003 (dotted line) and the same period in 2005 (solid line).

Service, Forest Inventory and Analysis (Clark et al., 2006). The ΔVI is defined as the ratio of a seasonally detrended vegetation index (VI) reduction before and after the hurricane and the seasonally detrended VI before the hurricane (Eq. (4)):

$$\Delta VI = \frac{(VI_{aug13} - VI_{sept14})}{VI_{aug13}} \tag{4}$$

In this study, the MODIS NBAR products observed on August 13, 2005 and September 14, 2005 were chosen as the observations before and after Hurricane Katrina, respectively. These observations are hereafter referred to as the observations before and after the hurricane. The ΔVIs derived from this period were referred to as ΔVIs_{2005}.

Then, we compared the statistical distributions of ΔVIs_{2005} with the ΔVIs derived from the observations on August 13 and September 14, 2003 (ΔVIs_{2003}) and the same periods in 2004 (ΔVIs_{2004}) and 2006 (ΔVIs_{2006}) over the same forest area within the major impacted region (severely and moderately damaged region, assessed by Clark et al. (2006)). We assumed that (1) ΔVIs_{2005} carried the forest damage information; and (2) ΔVIs_{2003}, ΔVIs_{2004}, and ΔVIs_{2006} represented the status of ΔVIs without major large-scale natural disturbances, since no hurricane landed or other large-scale ecosystem disturbances occurred in this region during those three years. The mean of ΔVIs ($\overline{\Delta VIs}$), shift amplitude (the difference of $\overline{\Delta VI}_{2005}$ and $\overline{\Delta VI}_{2003}$), statistical dispersion (Interquartile of Range (IQR) of ΔVIs_{2005}), and percentage of detected damaged forest pixels were calculated to evaluate the sensitivity of ΔVIs as post-hurricane damage indicators. The distribution of ΔVIs in 2003, 2004 and 2006 should have had a symmetric bell-shape distribution with $\overline{\Delta VIs}$ equal to or approximately 0, while ΔVIs in 2005 should have had a skewed distribution because of large-scale forest damage. Shift amplitude measures the sensitivity of an indicator to a hurricane's impact on the forest area. The shift amplitude increases when an indicator is more sensitive to forest damage. Statistical dispersion indicates the capability of an indicator to distinguish severity levels of the forest damage. An indicator with a large dispersion can better differentiate damage severity levels than other indicators. The percentage of damaged forest pixels that an indicator can detect is also indicative of that indicator's overall capability to detect forest damage.

4. Results and analysis

4.1. Post-hurricane damage indicator, ΔNDII

To visually compare the sensitivity of different indicators for detecting forest damage, the $\Delta NDII_{2005}$, $\Delta NDVI_{2005}$, ΔEVI_{2005}, ΔLAI_{2005} and $\Delta Fpar_{2005}$ are presented in Fig. 4(b)–(f), respectively. Fig. 4(a) presents a damage severity map reported by the USDA Forest Service (Clark et al., 2006), where the area within the black box represents the major impacted region. The major impacted region was later used to derive the statistical variables as presented in Fig. 5 and Table 2. The impacted region, used to derive damage thresholds, is the area within the red box in

Table 2
Statistics of ΔVIs in 2003 and 2005.

Statistical variables	ΔNDII	ΔNDVI	ΔEVI
% ΔVIs$_{2003}$ within [−0.4, 0.4]	99.3	99.9	99.3
% ΔVIs$_{2005}$ within [−0.4, 0.4]	96.8	99.9	99.4
$\overline{\Delta VIs}_{2003}$ (μ$_{2003}$)	−0.03	0.0	0.0
$\overline{\Delta VIs}_{2005}$ (μ$_{2005}$)	0.14	0.06	0.04
Shift amplitude	0.17	0.06	0.04
IQR of ΔVIs$_{2003}$	0.101	0.056	0.090
IQR of ΔVIs$_{2005}$	0.243	0.063	0.096
Damage threshold	0.04	0.02	0.03
% Damaged pixels	86.2	81.8	55.8

Fig. 6. Workflow of the rapid assessment algorithm.

Fig. 4(a). On Panels (b)–(f), the magenta line represents the hurricane track, and the red belt on the left is centered along Mississippi River, where the major land cover type is croplands. Because this study focused only on forested regions, it did not consider other land cover types. To facilitate comparison, the same scale was used – as shown in the color bars on Panels (b)–(f) – where green and blue represent the increase of vegetation indices after the hurricane, and yellow, orange and red indicate forest damage caused by the hurricane.

The most distinct feature of abrupt canopy modification detectable by optical remote sensing is the loss of green leaves, which should be directly correlated with a decrease in LAI, and indirectly correlated with a reduction of total chlorophyll and water content at the canopy level. However, Fig. 4 (e) and (f) showed that ΔLAI and ΔFpar could not detect the most impacted regions as shown in Panel (a). One of the reasons was that the MODIS Fpar product significantly underestimated the amplitude of ground Fpar change (Huemmrich et al., 2005). The hurricane impact identified by ΔNDII (Fig. 4b) was more consistent with damage severity assessed by the USDA Forest Service, Forest Inventory and Analysis (Clark et al., 2006) (Fig. 4(a)) than ΔNDVI (Fig. 4(c)) or ΔEVI (Fig. 4(d)). The impacted area (in yellow, orange and red) detected by ΔNDVI was smaller than ΔNDII, while ΔEVI underestimated the impacted area and did not differentiate the damage level as well as ΔNDII. Based on the above analysis, we found that ΔNDVI, ΔNDII and ΔEVI could detect post-hurricane forest damage to a certain extent, while ΔLAI and ΔFpar were unable to identify the most damaged forest regions. Therefore, we further analyzed only the statistical properties of ΔNDVI, ΔNDII and ΔEVI.

The histograms (Fig. 5) of ΔVIs within the major impacted region (within the black box in Fig. 4(a)) are ΔVIs distributions with or without the hurricane impact. These distributions were based on 13628 valid forest pixels within the ΔVIs range [−0.4, 0.4], which represented more than 99% of valid pixels, except for ΔNDII$_{2005}$ (96.8%). To facilitate the analysis, the histograms use lines instead of conventional bar charts to represent the distribution of ΔVIs. The relative decreases of the vegetation indices during the examined periods were represented by ΔVIs > 0. 0. The solid lines with filled marks are the histograms of ΔVIs$_{2005}$, which illustrate the distribution of ΔVIs after the hurricane. The dotted lines with hollow marks show the distributions of ΔVIs in 2003, which represent the distributions of ΔVIs without the impact of large-scale natural disturbances. The histograms of ΔVIs in 2004 and 2006 were similar to the ones in 2003, therefore we only presented the results from 2003 and 2005. The filled and hollow marks show the number of pixels within the corresponding intervals of ΔVIs, as they would be presented in the conventional histogram with bars. Fig. 5(b)–(d) shows, respectively, the mean of ΔVIs$_{2003}$ and ΔVIs$_{2005}$ (μ$_{2003}$ and μ$_{2005}$, respectively), the shift amplitude between ΔVI$_{2003}$ and ΔVI$_{2005}$ (μ$_{2005}$−μ$_{2003}$), the 25% and 75% quantiles of ΔVIs$_{2005}$, the Interquantile Range (IQR) of ΔVIs$_{2005}$, and the damage threshold. Fig. 5(a) includes the
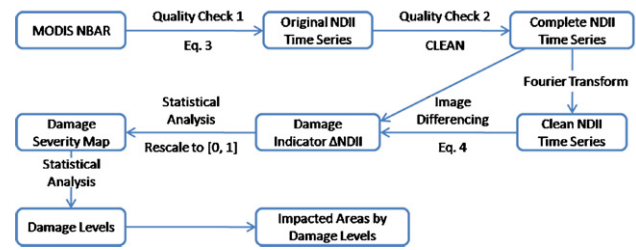
distributions of ΔVIs$_{2003}$ and ΔVIs$_{2005}$, as shown in Fig. 5(b)–(d), to ease the comparison among ΔNDII, ΔNDVI and ΔEVI. To analyze the distributions of the same ΔVI in 2003 and 2005 with the information of statistical properties, ΔNDII$_{2003,2005}$, ΔNDVI$_{2003,2005}$ and ΔEVI$_{2003,2005}$ are separately presented in Panels (b)–(d).

The histograms of ΔVIs$_{2003}$ (Fig. 5(a), dotted lines) had approximately a symmetric bell-shape distribution, with the mean (μ$_{2003}$ in Fig. 5(b)–(d), and $\overline{\Delta VIs}_{2003}$ in Table 2) equal to 0 or approximately 0, as shown in Table 2. This pattern of ΔVIs$_{2003}$ distribution was as expected because no large-scale natural disturbance was observed during August 13 and September 14, 2003. However, ΔVIs distributions in 2005 (Fig. 5(a), solid lines) shift to the direction of VIs decreasing when compared with the corresponding ΔVIs distributions in 2003. This reflects the impact of Hurricane Katrina, the only major large-scale disturbance observed in this region within the same period in 2005.

The shift amplitude was directly related to the sensitivity of these indices to hurricane impacts. The shift amplitude of ΔNDII (0.17) was greater than those of ΔNDVI and ΔEVI, as shown in Panels (b)–(d) and Table 2. The large shift amplitude of ΔNDII means the number of pixels with decreased NDII after the hurricane increased significantly, as shown in Panel (b). The shift amplitude of ΔNDVI (0.06) was slightly greater than the one of ΔEVI (0.04), but still insignificant when compared to the shift amplitude of ΔNDII.

The statistical dispersion (IQR) of ΔVIs$_{2005}$ (Table 2) indicated the sensitivity of an indicator to the damage severity levels. The large IQR of ΔNDII$_{2005}$ (0.24) implied the number of large ΔNDII values towards the right tail was greater than ΔNDVI and ΔEVI, so ΔNDII was more sensitive to the damage severity than other vegetation indices. The IQR of ΔNDII$_{2003}$ (0.101) was similar to that of ΔEVI$_{2003}$ (0.090), however, the IQR of ΔNDII$_{2005}$ (0.243) was much wider than that of ΔEVI$_{2005}$ (0.096). The IQR increase of
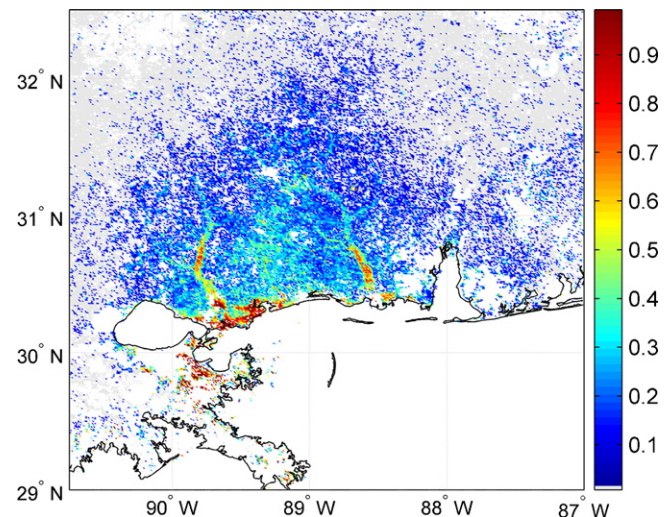

Fig. 7. Forest damage severity at the pixel level.

ΔNDII between 2003 and 2005 was 0.142, while the IQR increase of ΔNDVI and ΔEVI was insignificant (0.007 and 0.006, respectively). Less than 1% of the valid ΔVIs$_{2003}$ and ΔVIs$_{2005}$ were larger than 0.4 except for ΔNDII$_{2005}$, while more than 3% of the valid ΔNDII$_{2005}$ values were larger than 0.4 (Table 2). This further supports the finding that the effects of the hurricane not only shifted, but also stretched the ΔNDII2$_{005}$ distribution curve towards the positive direction more than it affected the other ΔVIs distributions.

The damaged pixels identified by ΔNDII were 86.2% of the total number of tree pixels within the major impacted region. This ratio was higher than what ΔNDVI and ΔEVI detected (81.8% and 55.8%,

respectively). Although both ΔNDII and ΔNDVI could detect close ratios of damaged forest pixels, ΔNDII had a more significant shift amplitude and a much wider range of IQR than ΔNDVI.

The above statistical analysis indicated that ΔNDII could detect hurricane-induced vegetation modification, in terms of total damaged forest, better than ΔLAI, ΔFpar, ΔEVI and ΔNDVI. This corroborated findings by visual inspection of ΔVIs maps of the hurricane-impacted region (Fig. 4), and confirmed previous findings that ΔNDII was a better indicator for detecting vegetation modification. The distributions of ΔNDVI, ΔEVI and ΔNDII were also analyzed for major forest types in this region, including
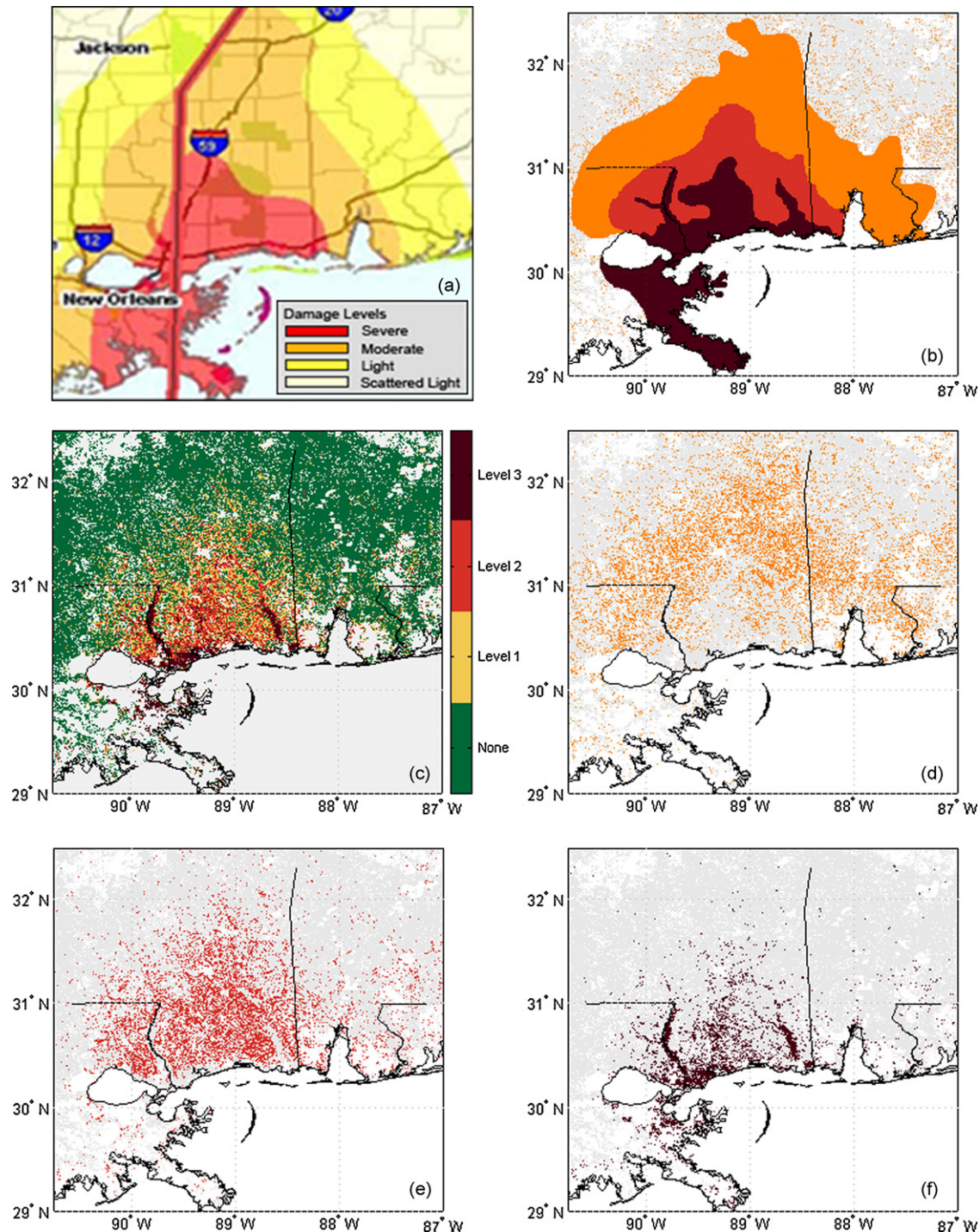
Fig. 8. Maps of forest damage levels (a) damage levels mapped by FIA, USDA Forest Service (Clark et al., 2006); (b) general damage map; (c) damage levels; (d) damage level 1; (e) damage level 2; and (f) damage level 3.

evergreen broadleaf forest, evergreen needle-leaf forest, deciduous broadleaf forest and mixed forest. The distributions for four major forest types had the same pattern as shown in Fig. 5.

4.2. Rapid assessment of post-hurricane forest damage

We developed a rapid post-hurricane forest damage assessment algorithm that comprised seven steps (Fig. 6). In Step 1, MODIS NBAR products that included at least 3 years of observations were checked to reject invalid or poor-quality observations using accessory quality flags. Then, reflectance at 0.86 and 2.13-μm channels was extracted and used to derive original NDII time series (Eq. (3)). In Step 2, the quality of original NDII time series was checked to eliminate anomalous high and low values, of which the next observations immediately return to approximately the previous values. The CLEAN algorithm was then used to estimate missing data, including abnormal high or low values, missing observations, and low quality observations. In Step 3, a Fourier transform technique was used to decouple seasonal signals and seasonally detrended disturbance signals, followed by Step 4, NDII image differencing (Eq. (4)). The damage indicator $\Delta NDII_{2005}$ was defined as the difference of seasonally detrended NDII pre- and post-hurricane divided by the complete NDII pre-hurricane. The damage indicator $\Delta NDII_{2005}$ was then rescaled to [0,1] to construct damage severity in Step 5. The upper and lower limits for rescale were decided by the statistical analysis of $\Delta NDII$. For example, an upper boundary 0.6 was selected, which covers 99.7% of valid $\Delta NDII_{2005}$ in the case of Hurricane Katrina impacts. A value of 0.6 was then assigned to pixels with $\Delta NDII_{2005}$ greater than 0.6. The lower boundary was the damage threshold, decided by the distribution of $\Delta NDII_{2003, 2004, 2006}$, as elaborated in Section 3.3. The damage severity was then stratified in Step 6 to identify the impacted areas by damage levels, which were determined through statistical analysis. In Step 7, damage areas were identified based on the spatial density and continuity of damaged forest pixels at individual damage levels.

This rapid assessment algorithm was applied to estimate forest damage after Hurricane Katrina. The forest damage severity map (Fig. 7) is the product of the algorithm at Step 5. It illustrates the distribution of forest damage on a scale of [0,1] at the pixel level. The pixels colored in light grey show no damage, while the other pixels colored in gradual blue, green, yellow and red represent damage in degrees from light to most severe. Although this map provided detailed damage information at the nominal 1 km^2 per pixel level, forest managers may need more general information to manage post-hurricane hazard relief activities.

A forest damage level map (Fig. 8(b)) can serve such a purpose. Fig. 8(a) is the distribution of forest damage levels estimated by the USDA Forest Service (Clark et al., 2006), where four levels were identified. Fig. 8(c) is the distribution of forest damage levels at the pixel level, derived from Step 6 of the rapid assessment algorithm. For the case of post-hurricane Katrina assessment, three levels were selected at first, including light (Level 1), moderate (Level 2) and severe (Level 3) damage, as shown in Fig. 8(c). Pixels without damage were in green, and those with land cover type other than forest were masked in grey. Pixels in the same damage level were mapped separately, as shown in Fig. 8(d) (light damage, orange), Fig. 8(e) (moderate damage, red) and Fig. 8(f) (severe damage, dark red). Based on the density and continuity of individual damage level maps, Fig. 8(b), a map of general damage levels was generated. The light damage level shown in Fig. 8(d) was separated into two levels, including light damage (orange belt in Fig. 8(b)) and scattered light damage (grey area with orange dots in Fig. 8(b)). Therefore, the general damage severity map had a total of four levels, i.e. scattered light, light, moderate and severe. Compared with Fig. 8(a), the area combining severely and

moderately damage areas in Fig. 8(b) was similar to the severely damage area estimated by the USDA Forest Service. The rapid assessment algorithm described in this paper was able to distinguish a new category of severity that represented the most severely damage area. The area with light damage in Fig. 8(b) was similar to the area with moderate damage in Fig. 8(a). The area in Fig. 8(b) with scattered light damage was comparable to the area combining the light and scatted light damage in Fig. 8(a).

5. Validation

The rapid assessment algorithm was validated using the ground truth data investigated by the USDA Forest Service, FIA. The forest damage estimated in the ground inventory for each plot was represented as the percentage of basal area that suffered no, light, moderate or severe damage. To validate the rapid assessment algorithm, the ground damage data were converted to the total damage severity (DS) for each plot using:

$$DS_i = \alpha_i \cdot \beta_i (\gamma_1 \cdot L_i + \gamma_2 \cdot M_i + \gamma_3 \cdot S_i + \gamma_4 \cdot N_i) \tag{5}$$

where DS_i stands for the total damage severity for the ith plot. The α_i is a tree size factor for the ith plot (Eq. (6)),

$$\alpha_i = \frac{(\text{mean tree DBH at } i\text{th plot})}{(\text{mean tree DBH of all plots})} \tag{6}$$

in which, DBH stands for the stem diameter at breast height. The β_i represents the effect of plot density for the ith plot (Eq. (7)),

$$\beta_i = \frac{(\text{tree density at } i\text{th plot})}{(\text{maximum tree density of all plots})} \tag{7}$$

The constants γ_1, γ_2, γ_3, and γ_4, are weight factors that measure the relative contribution of the four damage categories to the total damage severity. L_i, M_i, S_i and N_i are the percentage of basal area that suffered no, light, moderate or severe damage for the ith plot, respectively.

Using Eqs. (5)–(7), the total damage severity for 54 plots was derived. The $\Delta NDII_{2005}$ at these plots was retrieved using the nearest neighbor method. Despite the coarse damage categories used in the ground inventory, the scatter plot (Fig. 9) still showed a linear relationship between $\Delta NDII_{2005}$ and the total damage severity. This indicates that $\Delta NDII$ can quantitatively measure the damage severity of the hurricane-impacted forest region based on a strong linear relationship. The linear fitting line was $y = a + bx$,
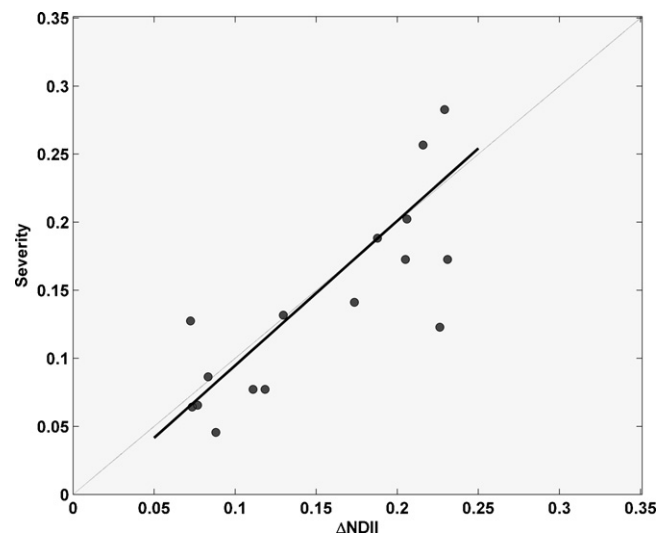

Fig. 9. The relationship of $\Delta NDII$ and the total damage severity. The dark grey dotted line is a 1:1 line.

where $a = -0.01$, $b = 1.06$, $r^2 = 0.79$, SD (standard deviation) = 0.03, p-value < 0.0001.

6. Conclusions

This study has developed a new approach for identifying forest regions impacted by hurricanes, and estimating damage severity. Using this approach, we have identified the impacted region and quantified the severity of forest damage post-Hurricane Katrina. The statistical analysis and comparison with the damage severity estimated by the USDA Forest Service revealed that ΔNDII was an optimal indicator for detecting hurricane-induced forest damage out of five commonly used vegetation indices, including NDVI, EVI, NDII, LAI and Fpar. Validation of this rapid assessment algorithm, compared with field measurements in the De Soto NF, showed a linear relationship between ΔNDII and the total damage severity with $r^2 = 0.79$ and p-value < 0.0001.

This study has shown that hurricane-induced forest damage severity can be quantified from satellite observed ΔNDII time series. However, ΔNDII presents primarily the change in total leaf water content in the forest canopy. The change of total chlorophyll content carried by the visible spectra is not considered in this algorithm. To improve the accuracy of this approach, an indicator that can integrate changes caused by total canopy chlorophyll and water content variations still needs to be investigated. The normalized damage severity (Fig. 7) represents the relative degrees of damage for a forest damage event. It is not suitable for comparison among various cases. However, the damage indicator ΔNDII, along with the forest type information, can be used to construct a standard damage severity scale for cross-case analysis. Additionally, the algorithm should be further validated by application to other areas to determine if it can be used in other vegetation types with dissimilar levels of damage. Because our damage thresholds were determined from the statistical properties of the data from the De Soto National Forest, it is likely that the thresholds in other forests would be different; such improvements could extend this approach to other post-disturbance assessments involving impacts on forest canopies such as insect or disease outbreaks or severe wildfire. The ability to assess degrees of damage, and not just mortality, would be beneficial in any schemes to compensate landowners for providing ecosystem services such as payments for carbon sequestration (Patenaude et al., 2005), for example Reduced Emissions from Deforestation and Degradation (REDD; see Zarin et al., 2009). This would benefit government decision processes by providing objective evidence for verifying post-hurricane compensation claims. For example, the European Union compensates member states for large-scale damage from wind and wildfire, and insurance schemes have been proposed to compensate individual landowners (Holecy and Hanewinkel, 2006). Providing that the MODIS NBAR product is available every 8 days, this algorithm is able to evaluate post-hurricane forest damage within a few weeks of an event.

Acknowledgements

References

Aosier, B., Kaneko, M., 2007. Evaluation of the forest damage by typhoon using remote sensing technique. In: IEEE International Conference on Geoscience and Remote Sensing Symposium, IGARSS 2007, Barcelona, Spain, July 23–27.

Ayala-Silva, T., Twumasi, Y.A., 2004. Hurricane Georges and vegetation change in Puerto Rico using AVHRR satellite data. International Journal of Remote Sensing 25 (9), 1629–1640.

Baisch, S., Bokelmann, G.H.R., 1999. Spectral analysis with incomplete time series: an example from seismology. Computers and Geosciences 25 (7), 739–750.

Boose, E.R., Foster, D.R., Fluet, M., 1994. Hurricane impacts to tropical and temperate forest landscapes. Ecological Monographs 64, 369–400.

Boutet Jr., J.C., Weishampel, J.F., 2003. Spatial pattern analysis of pre- and post-hurricane forest canopy structure in North Carolina, USA. Landscape Ecology 18, 553–559.

Bowyer, P., Danson, F.M., 2004. Sensitivity of spectral reflectance to variation in live fuel moisture content at leaf and canopy level. Remote Sensing of Environment 92, 297–308.

Bryant, D., Boykin, J., 2007. Fuels management on the National Forests in Mississippi after Hurricane Katrina. In: Butler, Bret W.; Cook, Wayne, comps. The fire environment—innovations, management, and policy; conference proceedings. 26–30 March 2007; Destin, FL. Proceedings RMRS-P-46CD. Fort Collins, CO: U.S. Department of Agriculture, Forest Service, Rocky Mountain Research Station. CD-ROM, pp. 287–292.

Ceccato, P., Flasse, S., Tarantola, S., Jacquemond, S., Gregoire, J.M., 2001. Detecting vegetation water content using reflectance in the optical domain. Remote Sensing of Environment 77, 22–33.

Chambers, J.Q., Fisher, J.I., Zeng, H., Chapman, E.L., Baker, D.B., Hurtt, G.C., 2007. Hurricane Katrina's carbon footprint on US gulf coast forests. Science 318, 1107.

Clark, J., Finco, M., Schwind, B., Megown, K., 2006. Rapid assessment of forest damage using multi-temporal Landsat TM imagery and high resolution aerial photography. In: 8th Annual Forest Inventory and Analysis Symposium, Monterey, California, October 16–19.

Coppin, P., Jonckheere, I., Nackaerts, K., Muys, B., Lambin, E., 2004. Digital change detection methods in ecosystem monitoring: a review. International Journal of Remote Sensing 25 (9), 1565–1596.

Dwyer, E., Pasquali, P., Holecz, F., Arino, O., 1999. Mapping forest damage caused by the 1999 Lothar Storm in Jura (France), using SAR Interferometry. ESA Earth Observation Quarterly 65, 28–29.

Floury, N., Toan, T.L., Souyris, J.C., Singh, K., Stussi, N., Hsu, C.C., Kong, J.A., 1997. Interferometry for forest studies. In: Proceedings of the Fringe 96 Workshop on ERS SAR Interferometry, ESA SP-406, vol. 2, December 1997, Zurich, Switzerland, September 30–October 2, 1996, pp. 57–70.

Foster, D.R., 1988. Species and stand response to catastrophic wind in central New England, USA. Journal of Ecology 76, 135–151.

Fransson, J.E., Walter, F., Blennow, K., Gustavsson, A., Ulander, L.M.H., 2002. Detection of storm-damaged forested areas using airborne CARABAS-II VHF SAR image data. IEEE Transactions on Geoscience and Remote Sensing 40 (10), 2170–2175.

Gardner, L.R., Michener, W.K., Blood, E.R., Williams, T.M., Lipscomb, D.J., Jefferson, W.H., 1991. Ecological impact of Hurricane Hugo-salinization of a coastal forest. Journal of Coastal Research 8, 301–317.

Gill, A.M., Moore, J.R.L., Cheney, N.P., 1990. Fires and their effects on the wet-dry tropics of Australia. In: Goldammer, J. (Ed.), Fire in the Tropical Biota: Ecological Studies. Springer, Berlin, pp. 159–178.

Hardisky, M.A., Lemas, V., Smart, R.M., 1983. The influence of soil salinity, growth form, and leaf moisture on the spectral reflectance of Spartina alternifolia canopies. Photogrammetric Engineering and Remote Sensing 49, 77–83.

Holecy, J., Hanewinkel, M., 2006. A forest management risk insurance model and its application to coniferous stands in southwest Germany. Forest Policy and Economics 8, 161–174.

Hook, D.D., Buford, M.A., Williams, T.M., 1991. The impact of Hurricane Hugo on the South Carolina coastal plain forest. Journal of Coastal Research 8, 291–300.

Huber, P., 1981. Robust Statistics. Wiley, New York.

Huemmrich, K.F., Privette, J.L., Mukelabai, M., Myneni, R.B., Knyazikhin, Y., 2005. Time-series validation of MODIS land biophysical products in a Kalahari woodland, Africa. International Journal of Remote Sensing 26 (19), 4381–4398.

Huete, A., Justice, C., Leeuwen, W.V., 1999. MODIS vegetation index (MOD13) algorithm theoretical basis document. Link: http://modis.gsfc.nasa.gov/data/atbd/atbd_mod 13.pdf.

Hunt, E.R., Rock, B.N., 1989. Detection of changes in leaf water content using near- and middle-infrared reflectances. Remote Sensing of Environment 30, 43–54.

Jacobs, D.M., 2007. Forest inventory, catastrophic events and historic geospatial assessment in the South. In: Proceedings of the American Society of Photogrammetry and Remote Sensing 2007 Annual Conference-Identifying Geospatial Solutions [CD-ROM], Society of Photogrammetry and Remote Sensing, Tampa, Florida, May 7–11.

Jasinski, M.F., 1990. Sensitivity of the normalized difference vegetation index to subpixel canopy cover, soil albedo, and pixel scale. Remote Sensing of Environment 32, 169–187.

Jin, S., Sader, S.A., 2005. Comparison of time-series tasseled cap wetness and the normalized difference moisture index in detecting forest disturbances. Remote Sensing of Environment 94 (3), 364–372.

Knyazikhin, Y., Martonchik, J.V., Myneni, R.B., Diner, D.J., Running, S.W., 1998a. Synergistic algorithm for estimating vegetation canopy leaf area index and fraction of absorbed photosynthetically active radiation from MODIS and MISR data. Journal of Geophysical Research 103, 32257–32276.

Knyazikhin, Y., Martonchik, J.V., Diner, D.J., Myneni, R.B., Verstraete, M., Pinty, B., Gobron, N., 1998b. Estimation of vegetation canopy leaf area index and fraction of absorbed photosynthetically active radiation from atmosphere-corrected MISR data. Journal of Geophysical Research 103 (D24), 32239–32256.

Kovacs, J.M., Blanco-Correa, M., Flores-Verdugo, F., 2001. A logistic regression model of hurricane impacts in a mangrove forest of the Mexican Pacific. Journal of Coastal Research 17 (1), 30–37.

Kupfer, J.A., Myers, A.T., McLane, S.E., Melton, G.N., 2008. Patterns of forest damage in a southern Mississippi landscape caused by Hurricane Katrina. Ecosystems 11, 45–60.

Lee, M., Lin, T., Vadeboncoeur, M.A., Hwong, J., 2008. Remote sensing assessment of forest damage in relation to the 1996 strong typhoon Herb at Lienhuachi Experimental Forest, Taiwan. Forest Ecology and Management 255, 3297–3306.

Liu, K., Lu, H., Shen, C., 2003. Assessing the vulnerability of the Alabama Gulf Coast to intense hurricane strikes and forest fires in the light of long-term climatic changes. In: Ning, Z.H., Turner, R.E., Doyle, T., Abdollahi, K.K. (Eds.), Integrated Assessment of the Climate Change Impacts on the Gulf Coast Region. The Gulf Coast Climate Change Assessment Council (GCRCC) and Louisana State University (LSU) Graphic Services, Baton Rouge, pp. 223–230.

Loope, L., Duever, M., Herndon, A., Snyder, J., Jansen, D., 1994. Hurricane impact on uplands and freshwater swamp forest. Bioscience 44, 238–246.

McNulty, S.G., 2002. Hurricane impacts on US forest carbon sequestration. Environmental Pollution 116, 17–24.

Meeker, J.R., Haley, T.J., Petty, S.D., Windham, J.W., 2006. Forest Health Evaluation of Hurricane Katrina damage on the De Soto National Forest. Report No. 2006-02-02, Forest Health Evaluation Alexandria Field Office, USDA Forest Service, Atlanta, GA.

Millward, A.A., Kraft, C.E., 2004. Physical influences of landscape on a large-extent ecological disturbance: the northeastern North American ice storm of 1998. Landscape Ecology 19, 99–111.

Miranda, M.L., 1996. Final report: an evaluation of the Post-Hugo forest recovery programs: salvage, wildfire hazard mitigation and reforestation. In: Haymond, J.L., Hook, D.D., Harms, W.R. (Eds.), Hurricane Hugo: South Carolina Forest Land Research and Management Related to the Storm. USDA Forest Service, General Technical Report SRS-5, pp. 498–532.

Myers, R.K., van Lear, D.H., 1998. Hurricane–fire interactions in coastal forests of the south: a review and hypothesis. Forest Ecology and Management 103, 265–276.

Patenaude, G., Milne, R., Dawson, T.P., 2005. Synthesis of remote sensing approaches for forest carbon estimation: reporting to the Kyoto Protocol. Environmental Science & Policy 8, 161–178.

Ramsey, E.W., Chappell, D.K., Baldwin, D.G., 1997. AVHRR imagery used to identify hurricane damage in a forested wetland of Louisiana. Photogrammetric Engineering and Remote Sensing 63 (3), 293–297.

Ramsey, E.W., Chappell, D.K., Jacobs, D.M., Sapkota, S.K., Baldwin, D.G., 1998. Resource management of forested wetlands: hurricane impact and recovery mapped by combining Landsat TM and NOAA AVHRR data. Photogrammetric Engineering and Remote Sensing 64 (7), 733–738.

Ramsey, E.W., Hodgson, M.E., Sapkota, S.K., Nelson, G.A., 2001. Forest impact estimated with NOAA AVHRR and Landsat TM data related to an empirical hurricane wind-field distribution. Remote Sensing of Environment 77, 279–292.

Roberts, D.H., Lehár, J., Dreher, J.W., 1987. Time series analysis with CLEAN. I. Derivation of a spectrum. Astronomical Journal 93 (4), 968–989.

Sader, S.A., Bertrand, M., Wilson, E.H., 2003. Satellite change detection of forest harvest patterns on an industrial forest landscape. Forest Science 49 (3), 341–353.

Schaaf, C.B., Gao, F., Strahler, A.H., Lucht, W., Li, X., Tsang, T., Strugnell, N.C., Zhang, X., Jin, Y., Muller, J.P., Lewis, P., Barnsley, M., Hobson, P., Disney, M., Roberts, G., Dunderdale, M., Doll, C., d'Entremont, R., Hu, B., Liang, S., Privette, J.L., 2002. First operational BRDF, Albedo and Nadir reflectance products from MODIS. Remote Sensing of Environment 83, 135–148.

Schlobohm, P., Brain, J., 2002. Gaining an Understanding of the National Fire Damage Rating System. National Wildfire Coordinating Group, National Interagency Fire Center, Boise. PMS 932, NFES 2665.

Sellers, P.J., 1985. Canopy reflectance, photosynthesis, and transpiration. International Journal of Remote Sensing 6, 1335–1372.

Sheffield, R.M., Thompson, M.T., 1992. Hurricane Hugo effects on South Carolina's Forest Resource. USDA Forest Service, Southeastern Forest Experiment Station Research Paper SE-284.

Stanturf, J.A., Goodrick, S.L., Outcalt, K.W., 2007. Disturbance and coastal forests: a strategic approach to forest management in hurricane impact zones. Forest Ecology and Management 250, 119–135.

Stueve, K.M., Lafon, C.W., Isaacs, R.E., 2007. Spatial patterns of ice storm disturbance on a forested landscape in the Appalachian Mountains, Virginia. Areas 39 (1), 20–30.

Tucker, C.J., 1979. Red and photographic infrared linear combinations for monitoring vegetation. Remote Sensing of Environment 8, 127–150.

Wade, D.D., Forbus, J.K., Saveland, J.M., 1993. Photo Series for Estimating Post-hurricane Residues and Fire Behavior in Southern Pine. USDA Forest Service, Southeastern Forest Experiment Station General Technical Report SE-82.

Wang, F., Xu, Y., 2009. Hurricane Katrina-induced forest damage in relation to ecological factors at landscape scale. Environmental Monitoring and Assessment 156 (1–4), 491–507.

Wang, L., Qu, J.J., Xiong, J., Hao, X., Xie, Y., Che, N., 2006. A new method for retrieving Band 6 of Aqua MODIS. IEEE Geoscience and Remote Sensing Letters 3 (2), 267–270.

Wiesmann, A., Wegmüller, U., Honikel, M., Strozzi, T., Werner, C.L., 2001. Potential and methodology of satellite based SAR for hazard mapping. In: Proceedings of Geoscience and Remote Sensing Symposium, IGARSS 2001, Sydney, Australia, July 9–13.

Wilson, E.H., Sader, S.A., 2002. Detection of forest type using multiple dates of Landsat TM imagery. Remote Sensing of Environment 80, 385–396.

Windham, J.W., 2005. Forest vegetation analysis, Hurricane Katrina damaged tree removal and hazardous fuels treatment. USDA Forest Service, Link: http://www.fs.fed.us/r8/mississippi/katrina/EA/Supporting_Documentation/Katrina_Forest_Vegetation_Analysis.pdf (last accessed 10/22/2008).

Zarin, D., Angelsen, A., Brown, S., Loisel, C., Peskett, L., Streck, C. 2009. Reducing Emissions from Deforestation and Forest Degradation (REDD): An Options Assessment Report. Prepared for the Government of Norway. Meridian Institute, available online at http://www.REDD-OAR.org.

Zhang, X., Friedl, M.A., Schaaf, C.B., Strahler, A.H., Hodges, J.C.F., Gao, F., Reed, B.C., Huete, A., 2003. Monitoring vegetation phenology using MODIS. Remote Sensing of Environment 84, 471–475.